SPANDIDOS PUBLICATIONS

INTERNATIONAL JOURNAL OF MOLECULAR MEDICINE 45: 1803-1813, 2020

miR-181b-p53 negative feedback axis regulates osteosarcoma cell proliferation and invasion

JUN WAN, FENG LONG, CAN ZHANG and YUPENG LIU

Department of Orthopaedics, Xiangya Hospital, Central South University, Changsha, Hunan 410008, P.R. China

Received June 17, 2019; Accepted January 21, 2020

DOI: 10.3892/ijmm.2020.4558

Abstract. Osteosarcoma (OS) is one of the most common malignant tumors in young adults and has a high distant metastasis rate. The p53 protein, a potent prognostic biomarker for patients with OS, is altered in ~50% of OS cases. p53 was reported to exert its effects through regulating the transcription of microRNAs (miRNAs/miRs) and other genes. In the present study, the expression of miR-181b, a critical OS oncomiR, was shown to be significantly upregulated whereas p53 expression was downregulated within OS tissues and cells; in tissue samples, miR-181b and p53 were negatively correlated. p53 inhibited the transcription of miR-181b via targeting its promoter region, whereas miR-181b bound the *TP53* 3'-untranslated region (UTR) to inhibit p53 expression. miR-181b silencing considerably increased p53, p21, and epithelial-Cadherin protein levels but decreased Cyclin D1 protein levels in OS cells. In addition, miR-181b inhibition reduced OS cell proliferation and invasion. In contrast, p53 knockdown had the opposite effects on these proteins and OS cell proliferation and invasion. Above all, p53 knockdown significantly attenuated the effects of miR-181b inhibition. Moreover, OS cell xenograft assays further confirmed the roles of the miR-181b/p53 axis in OS growth. In conclusion, miR-181b and p53 are negatively regulated by one another and therefore form a negative feedback axis that regulates the proliferation and invasion abilities of OS cells. Targeting miR-181b to inhibit its abnormal upregulation might be a potent strategy for OS treatment.

Introduction

Osteosarcoma (OS) represents ~60% of malignant bone tumors (1) and mostly occurs in young adults. The high distant metastatasis rate of OS leads to limited survival in OS patients, particularly terminal patients or patients with multidrug resistance (2,3). Therefore, the need to explore the potential molecular mechanism of OS to not only develop complementary or alternative treatments but also enhance the therapeutic effects of current treatments is urgent.

Over the past few years, the medical community has paid great attention to the potential of gene treatment and targeted therapy in elucidating the mechanisms of disease and altering diseases at the molecular level (4). The identification of specific genes can be essential for success. *TP53*, which is commonly regarded as one of the most critical tumor suppressor genes, serves as a central regulatory factor in cell proliferation, cell apoptosis and other biological processes (5-8). The p53 protein prevents the proliferation of injured or mutated cells by inducing cell cycle arrest, apoptosis or senescence; therefore, the p53 dysfunction might promote the generation and development of tumors (9-11). Interestingly, it was reported that *TP53* could act as a potential prognostic biomarker for patients with OS (12,13) and was altered in ~50% of OS cases (12). Zhao *et al* (14) revealed that the overexpression of p53 enhanced the chemical sensitivity of multidrug-resistant OS cell lines, while Wu *et al* (15) demonstrated that the expression of p53 has emerged as a valid prognostic biomarker for predicting the survival of OS patients. Fully understanding its functional network will be of great benefit to clinical treatment.

Located at the center of a complex molecular regulatory network, *TP53* can induce cell cycle arrest and apoptosis via regulating the transcription of microRNAs (miRNAs/miRs) and other different genes. miRNAs play a crucial role as post-transcriptional regulatory factors that bind target mRNAs at their 3' untranslated region (UTR) to repress gene expression (16-18). Previously, Jones *et al* (19) regarded the miR-181 group as an essential OS oncomiR; three of the four miRNAs from the miR-181 group, including miR-181a, miR-181b and miR-181c, were highly upregulated within OS samples (19). Furthermore, miR-181 can activate the Wnt signaling pathway (20), which is essential for the pathogenesis of OS (21). miR-181a (22,23) and miR-181b (24,25) both promote the capacity of cells proliferation and invasion but inhibit OS cell apoptosis. More notably, based on online predictive tools, p53 might bind miR-181b at its promoter region, while miR-181b might target *TP53* at its 3'-UTR to negatively regulate one another. Therefore, the present study hypothesized that the abnormal upregulation of miR-181b in OS disturbs the negative feedback balance between p53 and miR-181b, causing excessive OS cell proliferation and invasion.

Correspondence to: Professor Yupeng Liu, Department of Orthopaedics, Xiangya Hospital, Central South University, 87 Xiangya Road, Changsha, Hunan 410008, P.R. China
E-mail: yupengliu510@sina.com

Key words: osteosarcoma, miR-181b, p53, proliferation, invasion

In the present study, miR-181b and p53 expression was determined in normal noncancerous and OS tissue samples; then the correlation between miR-181b and p53 expression in tissues was examined. Next, the predicted interactions between p53 and miR-181b promoter and between miR-181b and the *TP53* 3'-UTR and the negative regulation of miR-181b and p53 were verified. Moreover, the full effects of miR-181b on p53 signaling and the proliferation, and invasion of OS cells and the dynamic effects of miR-181b and p53 on OS cells were evaluated *in vitro* and *in vivo*. In summary, the present study provides a mechanism by which the miR-181b-p53 negative feedback axis affects the proliferation and invasion of OS cells.

Materials and methods

Clinical tissue samples. OS tissues and adjacent normal noncancerous tissues (n=12, each) were collected during routine therapeutic surgery at Xiangya Hospital from Feburay, 2018 to Feburay, 2019. (F/M is 3/9, the average age is 24.33±7.10 years). OS patients who participated in this study had been not received chemotherapy or radiotherapy. Inclusion criteria and exclusion criteria were adopted from previous studies (26,27). The adjacent normal noncancerous tissues were 5 cm distance from OS tissues. All tissue specimens were frozen in liquid nitrogen immediately and stored at -80˚C until use. The present study was reviewed and approved by the Ethics Committee of Xiangya Hospital and each patient signed an informed consent document.

Cell lines and cell transfection. Primary human osteoblasts (HOBs) were obtained from Merck KGaA (cat. no. 406-05F) and cultured in a 1:1 mixture of Ham's F12 medium and Dulbecco's modified Eagle's medium (both from Gibco; Thermo Fisher Scientific, Inc.), with 2.5 mM L-glutamine (without phenol red) and 10% fetal bovine serum (FBS) (Gibco; Thermo Fisher Scientific, Inc.). A total of two OA cell lines, U2OS (American Type Cututre Collection; ATCC HTB-96™) and MG63 (ATCC CRL-1427™) cells were obtained from ATCC. U2OS cells were cultured in McCoy's 5a medium (cat. no. 30-2007; ATCC) supplemented with 10% FBS. MG63 cells were cultured in Eagle's Minimum essential medium (cat. no. 30-2003; ATCC) supplemented with 10% FBS. Cells were cultured at 37˚C in 5% CO_2.

For cell transfection, 20 nM negative control (NC) mimics and miR-181b-5p mimics, 20 nM NC inhibitor and miR-181b-5p inhibitor, 1 μg/ml control vector and p53-overexpression vector (p53 OE), or 20 nM small intereferring (si)-NC and si-p53 that had been designed and purchased from Shanghai GenePharma Co., Ltd., were used. Cells in log phase were seeded into 12-well plates at a density of $5x10^5$ cells/ml one day before transfection. When the cell confluence reached 70%, siRNAs, vectors and miRNA mimics or inhibitors were diluted in Opti-MEM (Invitrogen; Thermo Fisher Scientific, Inc.) and incubated with 5 μl Lipofectamine 2000 (Invitrogen; Thermo Fisher Scientific, Inc.) for 5 min at room temperature. Next, the DNA-lipid complex were added to cells. Then, cells were incubated at 37˚C in a CO_2 incubator. Medium was then replaced with fresh complete medium containing 10% FBS after 6 h of transfection. A total of 48 h after transfection, cells were harvested for further experiments. The sequence of miRNA mimics or inhibitor and primers for plamid construction were listed in Table SI.

PCR-based analyses. Total RNA from tissues or target cells was extracted using TRIzol reagent (Invitrogen; Thermo Fisher Scientific, Inc.), following the manufacturer's procedures. A NanoDrop-1000 (Thermo Fisher Scientific, Inc.) was used to determine concentrations and for quality control purposes. Complementary DNA was synthesized from extracted RNA 9 (5 μg) using the Prime Script® RT Reagent kit with gDNA Eraser (Invitrogen; Thermo Fisher Scientific, Inc.) in accordance with the recommended protocol (samples and reagent mix were incuabated at 37˚C for 15 min and 85˚C for 5 sec, and finally stored at 4˚C). Quantitative (q)PCR was performed using SYBR®Premix Ex Taq™ II (Invitrogen; Thermo Fisher Scientific, Inc.). ABI7500 real-time PCR detection system (Applied Biosystems; Thermo Fisher Scientific, Inc.) was used for detection. The qPCR thermocycling conditions were as follows: The initial denaturation was first performed at 95˚C for 2 min followed by denaturation at 95˚C for 15 sec and annealing and extension at 60˚C for 30 sec. Repeat the denaturation, annealing and extension for 40 circles. After amplification, data were collected and processed by the comparative cycle threshold method. U6 and GAPDH expression levels were used as internal references for miRNA and mRNA expression detection, respectively. Finally, the data were processed using the $2^{-\Delta\Delta Cq}$ relative expression method (28). The primers were listed in Table SI.

Chromatin immunoprecipitation (ChIP) analysis. Target cells were suspended in 1% formaldehyde in PBS, cross-linked for 10 min at room temperature, washed twice with PBS and lysed with SDS lysis buffer (Promega Corporation). At 4˚C, the lysates were centrifuged at 1,0000 x g for 10 min; the supernatants were diluted with ChIP dilution buffer (EMD Millipore) and then immunoprecipitated using an anti-p53 antibody (cat. no. ab1101; 1:20) or mouse IgG (cat. no. ab190475; 1:20) (both from Abcam). IgG served as a negative control. The immunoprecipitated DNA was then analyzed by qPCR.

Luciferase reporter assay. To test the relationship between TP53 and miR-181b, the online tool LncTar (http://www.cuilab.cn/lnctar) was used to predicate the biding site between TP53 3'UTR and miR-181b-5p. Then, dual-luciferase reporter assay was carried out. First, TP53 3'-UTR was cloned into the downstream of the psiCheck2 vector (Promega Corporation) to generate the wild-type TP53 3'-UTR luciferase reporter vector; a mutant TP53 3'-UTR luciferase reporter vector was generated by mutating the predicted miR-181b-binding site within the TP53 3'-UTR. These two reporter vectors were cotransfected with miR-181b mimics or miR-181b inhibitor into 293T cells (ATCC). A total of 48 h later, the cells were harvested and underwent a dual-luciferase reporter assay (Promega Corporation) to evaluate firefly and *Renilla* the luciferase activities. *Renilla* luciferase activity served as a normalization control.

Immunoblotting. The cell lysates of OS cell lines were prepared using RIPA lysis buffer (Beyotime Institute of Biotechnology), and a bicinchoninic acid protein assay kit

(Pierce; Thermo Fisher Scientific, Inc.) was used to detect protein concentration. The 30-50 μg protein samples were then separated by 10-15% SDS-PAGE and transferred onto PVDF membranes (Thermo Fisher Scientific, Inc.). The membranes were blocked with 5% non-fat milk in TBST (0.1% Tween-20) for 2 h at room temperature and incubated with primary antibodies against p53 (1:1,000; cat. no. ab26; Abcam), p21 (1:1,000; cat. no. ab109520; Abcam), Cyclin D1 (1:1,000; cat. no. ab16663; Abcam), epithelial (E)-cadherin (1:1,000; cat. no. ab1416; Abcam) and GAPDH (1:2,000; cat. no. ab8245; Abcam) overnight at 4˚C. After washing three times with TBST, the membranes were incubated for 1 h with goat-anti-rabbit or goat-anti-mouse HRP antibody (both 1:5,000; cat. nos. ab205718 and ab205719; both from Abcam) at room temperature. Intensity analyses were performed using ImageJ software version 1.8.0 (National Institute of Health).

Cell viability determined by MTT assay. Cells were seeded in 96-well plates at a density of $5x10^3$/well and transfected or treated. A total of 48 h later, MTT solution (20 μl; 5 mg/ml) was added to the plates at the 0, 12, 24 and 48 h and incubated at 37˚C for 4 h. At the end of the incubation, dimethyl sulfoxide was added to lyse the cells and the supernatant was subsequently removed. Then the absorbance value at 490 nm was measured.

DNA synthesis determined by 5-ethynyl-2'-deoxyuridine (EdU) assay. The ability to synthesize DNA was detected by EdU assays using an EdU assay kit (Guangzhou RiboBio Co., Ltd.) following a previously described method (29). Nuclei were stained with DAPI for 15 min at room temperature. Representative images were taken under an IX71 fluorescence microscope (Olympus Corporation). A total of five random fields were analyzed per sample.

Cell invasion determined by Transwell assay. Treated OS cells ($1x10^5$ cells) were suspended in serum-free medium in 24-well Transwell chambers precoated with Matrigel; medium containing 10% FBS was added to the bottom chamber. After cultured for 48 h at 37˚C in a CO_2 incubator, noninvasive cells in the upper chambers were discarded whereas invasive cells were fixed with 5% paraformaldehyde for 20 min at room temperature and then stained with 0.1% crystal violet for 20 min at room temperature. Invasive cells were in 4 random fields in each group were counted under a light microscope (magnification x200) (Olympus).

Establishment of xenograft nude mice. Antagomir-miR-181b, antagomir-NC, p53 short hairpin (sh)RNA plasmid (sh-p53) and NC shRNA plasmid (sh-NC) were obtained from Shanghai GenePharma Co., Ltd. Antagomir-miR-181b, antagomir-NC sh-p53 or sh-NC was transfected into MG63 cells with Lipofectamine 2000. A total of 48 h later, the transfected cells were harvested for subcutaneous injection. To establish a human OS cell xenograft nude mouse model, a total of 24 female nude mice (BALB/c-nu/nu) at 6-week-old and weighing 16-20 g were obtained from the SLAC Laboratory Animal Center. The mice were housed in specific pathogen-free room (22˚C, ~50% humidity) and fed a standard irradiated diet and had unrestricted access to purified water. Mice were maintained on a 12-h light cycle. A total of 24 mice were randomly divided into the following 4 groups: An antagomir-NC+sh-NC group, antagomir-miR-181b+sh-NC group, antagomir-NC+sh-p53 group and antagomir-miR-181b+sh-p53 group. A total of $1x10^6$ transfected MG63 cells were suspended in 100 μl PBS and subcutaneously injected into the right anterior armpits of the nude mice. A total of 28 days later, mice were anesthetized via the respiratory route by exposing them to ether for 2 min in a transparent acrylic jar. The depth of anesthetization was sufficient when the following vital criteria are reached: Regular spontaneous breathing. No reflex after the setting of pain stimuli between toes and no response to pain. Then, mice were sacrificed by cervical dislocation. The tumor weight and volume were meausured. The animal epxeriments were approved by the Ethic Committee of Xiangya Hospital of Central South University.

Statistical analysis. All data from at least three independent experiments were processed using GraphPad software (version 7; GraphPad Prism), and are presented as the mean ± standard deviation. Differences between two groups were determined using both unpaired or paired Student's t-test where appropriate, and following one-way analysis of variance, Tukey's test was used for comparison among three groups or more. For the correlation analysis, the Pearson correlation coefficient analysis was used. $P<0.05$ was considered to indicate a statistically significant difference.

Results

miR-181b and p53 expression within OS tissue samples and cell lines. First, miR-181b and p53 expression was verified within tissues and cell lines. Fig. 1A and B show that the expression of miR-181b was significantly upregulated, while p53 expression was downregulated within OS tissue samples compared with noncancerous tissue samples. Pearson correlation coefficient analysis showed that miR-181b expression was negatively correlated with p53 expression in OS tissue (Fig. 1C). Consistently, miR-181b expression was upregulated and p53 expression was downregulated in two OS cell lines, MG63 and U2OS, compared with normal HOBs (Fig. 1D and E).

p53 inhibits the transcription of miR-181b in OS cells. To verify the predicted binding between p53 and the miR-181b promoter region, the MG63 and U2OS cell lines were transfected with p53 OE or si-p53 vector for p53 OE or p53 knockdown, respectively, and qPCR was performed to verify the transfection efficiency (Fig. 2A). Next, miR-181b expression was determined in p53-overexpressing or p53-silenced OS cells; p53 OE significantly inhibited miR-181b expression, whereas p53 knockdown significantly promoted miR-181b expression in both OS cell lines (Fig. 2B). To provide further evidence of the predicted binding of p53 to the miR-181b promoter (Fig. 2C), ChIP assays were performed with anti-p53 and anti-IgG antibodies. Fig. 2D shows that the relative abundance of the miR-181b promoter precipitated by anti-p53 was significantly increased compared with precipitated with anti-IgG, especially in p53-overexpressing 293T cells, indicating that p53 can inhibit the expression of miR-181b via targeting its promoter region.

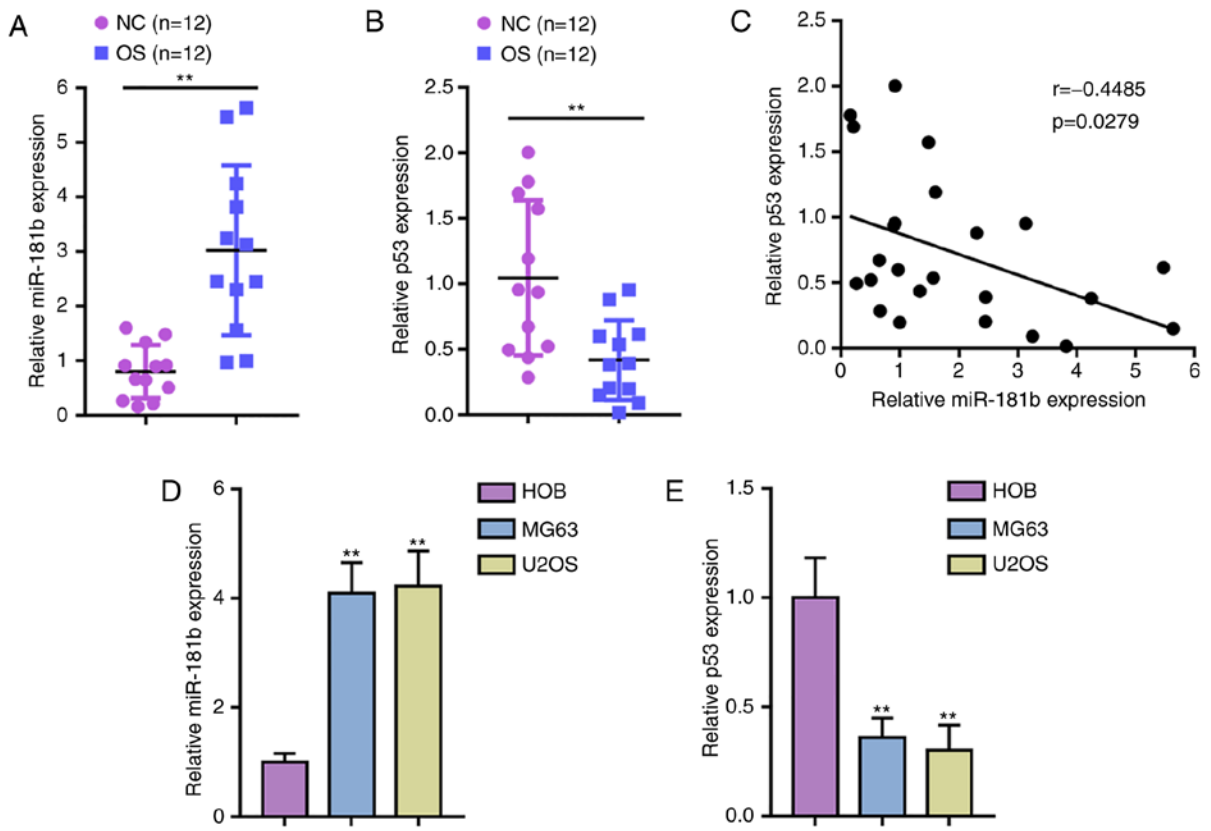

Figure 1. miR-181b and p53 expression in OS tissues and cell lines The expression of (A) miR-181b and (B) p53 in noncancerous and OS tissue samples was determined by qPCR. (C) The correlation between miR-181b and p53 expression in OS tissue samples. The expression of (D) miR-181b and (E) p53 in normal HOBs and two OS cell lines U2OS and MG63 cells, was determined by qPCR. **P<0.01. miR, microRNA; OS, osteosarcoma; NC, negative control; q, quantitative; HOBs, human osteoblasts.

miR-181b suppresses the expression of p53 via targeting its 3'-UTR. The online tool LncTar predicted that miR-181b might target p53 3'-UTR. To verify this prediction, miR-181b mimic or inhibitor were transfected to induce miR-181b OE or inhibition, respectively, within the MG63 and U2OS cell lines, and performed qPCR to confirm the transfection efficiency (Fig. 3A). Consistent to the prediction, p53 expression was inhibited via miR-181b OE while expression was promoted via miR-181b inhibitor transfection (Fig. 3B). To verify this interaction, two luciferase reporter vectors were constructed, wild-type and mutant TP53 3'-UTR luciferase reporter vectors, that contained the wild-type or mutated miR-181b binding site, respectively (Fig. 3C). These reporter vectors were transfected into 293T cells with the miR-181b mimic/inhibitor and the luciferase activity was examined. Fig. 3D shows that the luciferase activity of cells transfected with the wild-type TP53 3'-UTR vector was reduced via the OE of miR-181b but increased via the inhibition of miR-181b; mutation of the putative miR-181b binding site within TP53 3'-UTR could abolish the alterations in the luciferase activity. In summary, miR-181b can suppress the expression of TP53 via direct binding to its 3'-UTR.

Detailed effects of miR-181b on p53 signaling and OS cell proliferation and invasion. After confirming the binding between p53 and the miR-181b promoter and miR-181b and the *TP53* 3'-UTR, the specific effects of miR-181b on p53 signaling and OS cells were determined. The MG63 and U2OS cell lines were transfected with miR-181b inhibitor and then examined p53, p21, Cyclin D1, and E-cadherin protein levels. In both cell lines, miR-181b inhibition dramatically increased p53, p21 and E-cadherin protein levels, but decreased the protein levels of Cyclin D1 (Fig. 4A). The MTT assay showed that the miR-181b inhibitor decreased the proliferative potential of the MG63 and U2OS cell lines (Fig. 4B). Similarly, miR-181b inhibition also decreased the ability of OS cells to synthesize DNA (Fig. 4C). Finally, the Transwell assay indicated that metastatic ability of OS cells was significantly restricted by the miR-181b inhibitor (Fig. 4D). In summary, miR-181b inhibition enhanced p53 signaling activation. Consistently, miR-181b inhibition reduced cell viability, DNA synthesis and the invasive ability of both OS cell lines.

Dynamic effects of miR-181b and p53 on the proliferation and invasion of OS cells. After confirming the full impact of miR-181b on p53 signaling and OS cell lines, whether miR-181b brings about these effects via targeting p53 was determined. The MG63 and U2OS cell lines were cotransfected with miR-181b inhibitor and si-p53 and then miR-181b and p53 expression was evaluated. miR-181b expression was dramatically reduced via miR-181b inhibitor transfection but increased via si-p53 transfection; miR-181b inhibitor transfection significantly attenuated the effect of si-p53 (Fig. 5A). Conversely, p53 expression was considerably increased via miR-181b inhibition but reduced via si-p53 transfection; the effects of the miR-181b inhibitor were significantly attenuated

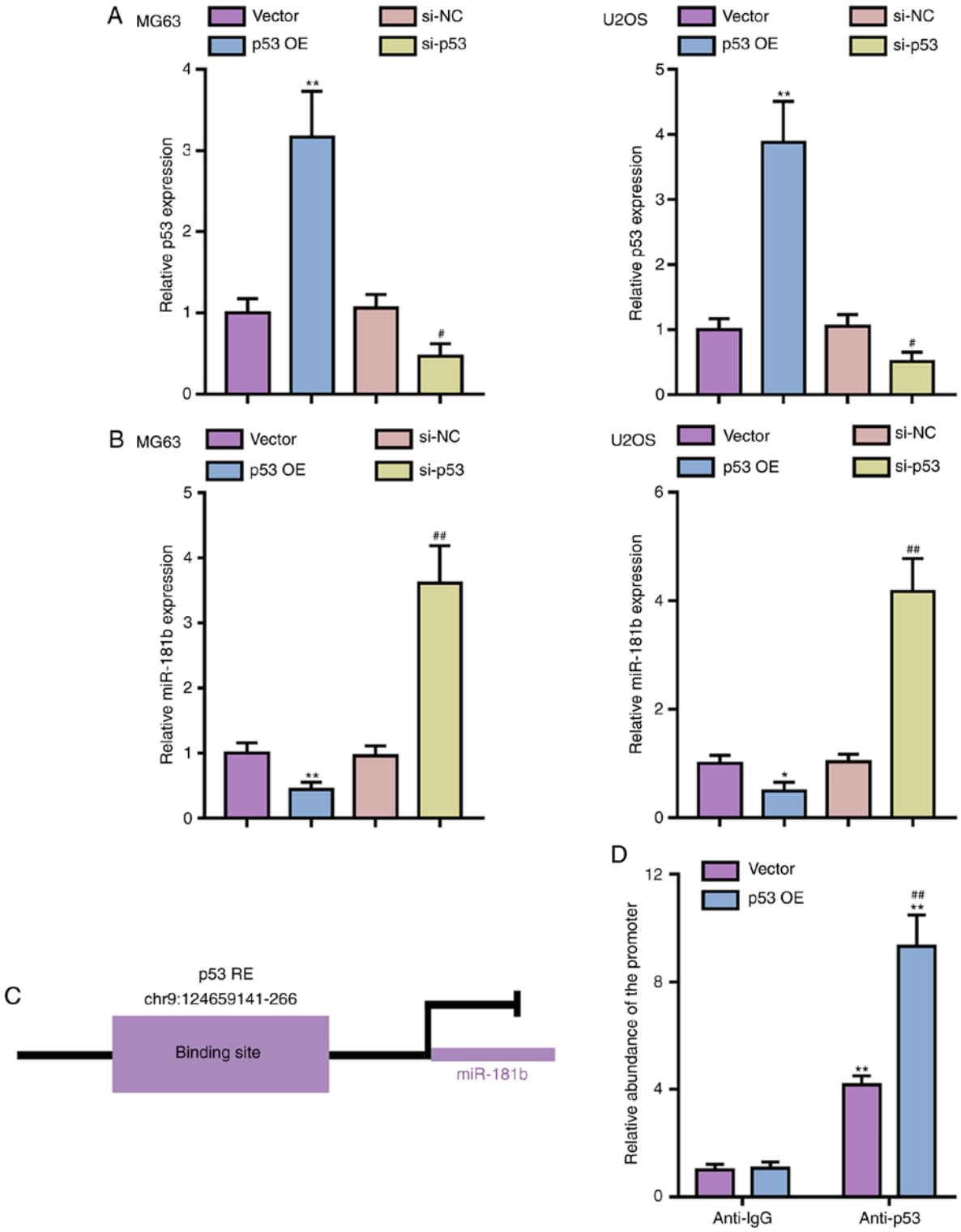

Figure 2. p53 inhibits the transcription of miR-181b in OS cells. (A) p53 OE or knockdown was carried out in MG63 and U2OS cells by the transfection of p53 OE vector or si-p53, as confirmed by qPCR. (B) miR-181b expression in response to p53 OE or knockdown in MG63 and U2OS cells was determined by qPCR. *P<0.05 and **P<0.01 vs. the vector group; $^{\#}$P<0.05 and $^{\#\#}$P<0.01 vs. the si-NC group. (C) A schematic diagram showing the predicted p53-binding site on the miR-181b promoter. (D) Chromatin immunoprecipitation assays were performed with anti-p53 and anti-IgG antibodies; the abundance of miR-181b promoter precipitated with anti-p53 and anti-IgG antibodies was determined in 293T cells transfected with NC or p53 OE vector. **P<0.01 vs. the anti-IgG group; $^{\#\#}$P<0.01 vs. the anti-p53 + NC group. NC, negative control; OS, osteosarcoma; miR, microRNA; q, quantitative; si, small interfering; Ig, immunoglobulin; OE, overexpression.

via si-p53 transfection (Fig. 5B). These data further confirm that miR-181b and p53 are negatively regulated by each other.

Regarding the p53 signaling, the protein levels of p53, p21 and E-cadherin were significantly increased by miR-181b inhibitor transfection and decreased by si-p53 transfection; on the contrary, Cyclin D1 was reduced by miR-181b inhibition and raised by p53 knockdown (Fig. 5C). p53 knockdown significantly attenuated the effects of miR-181b inhibition

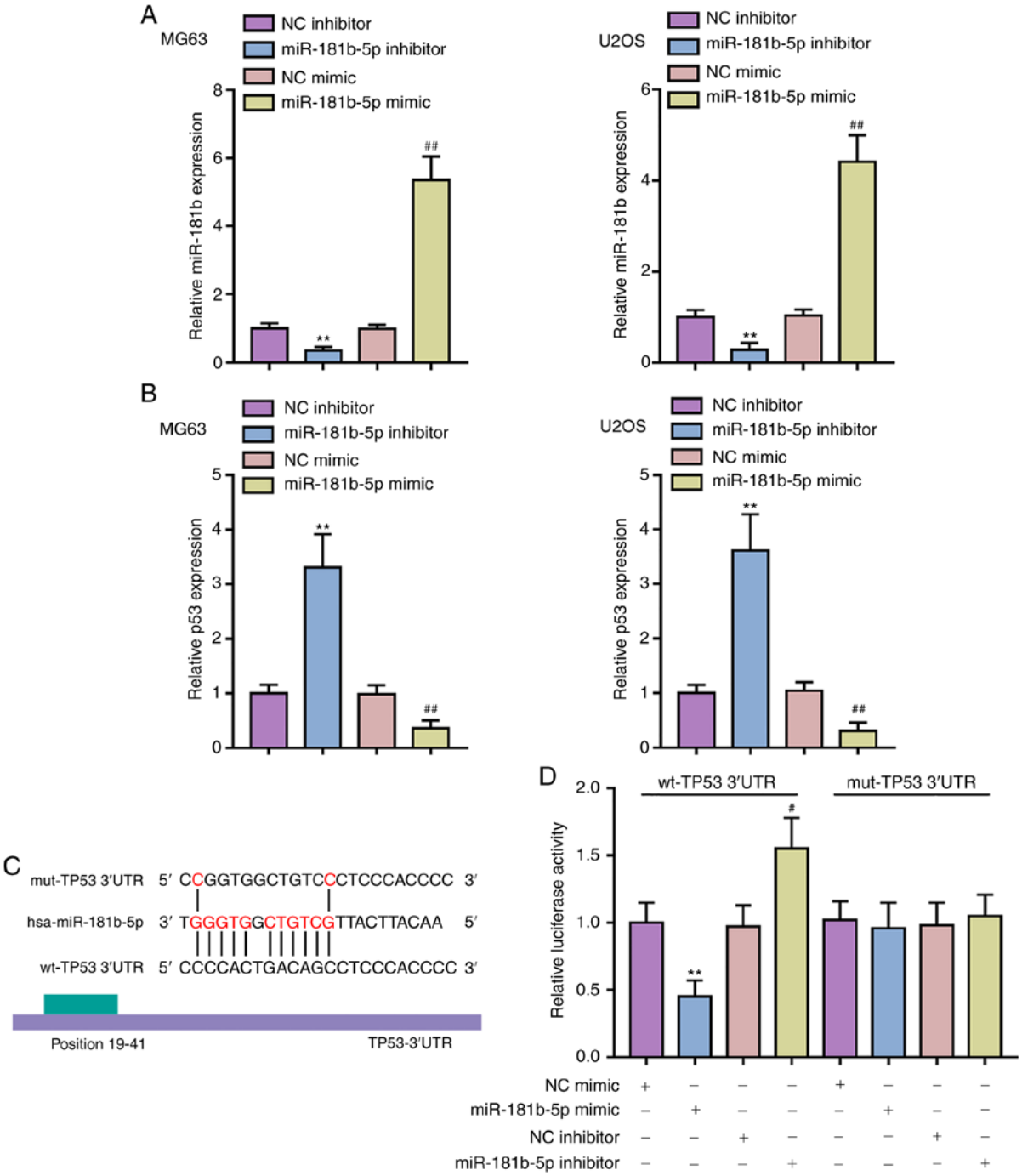

Figure 3. miR-181b binds the 3'-UTR of p53 to inhibit its expression. (A) miR-181b OE and inhibition was carried out in MG63 and U2OS cells by the transfection of miR-181b mimic or miR-181b inhibitor, respectively, as confirmed by qPCR. (B) p53 expression in response to miR-181b OE or miR-181b inhibition was determined in MG63 and U2OS cells by qPCR. **P<0.01, vs. the NC inhibitor group; $^{\#}$P<0.05 and $^{\#\#}$P<0.01 vs. NC mimic group. (C) A schematic diagram showing the predicted binding site of miR-181b in TP53 3'-UTR. Wt and mut TP53 3'-UTR luciferase reporter vectors were constructed as described in the Materials and methods section. (D) These reporter vectors were co-transfected in 293T cells with miR-181b mimic or miR-181b inhibitor and luciferase activities were determined. UTR, untranslated; miR, microRNA; NC, negative control; q, quantitative; wt, wild-type; mut, mutant; OE, overexpression.

(Fig. 5C). Consistently, miR-181b inhibition significantly suppressed, whereas p53 knockdown promoted cell viability, DNA synthesis and the invasive abilities of both OS cell lines (Fig. 5D-F). These data indicate that miR-181b functions in OS cells via targeting p53 and thus affecting p53 signaling.

Dynamic effects of miR-181b and p53 on OS cell xenograft nude mice. To further validate the effects of miR-181b and p53 *in vivo*, an OS cell xenograft model was established in nude mice using antagomir-181b transfected and/or p53 knockdown MG63 cells. As shown in Fig. 6A and B, antagomir-miR-181b transfection significantly decreased the tumor weight and volume, and these changes were reversed by p53 knockdown. The protein levels of p53, p21 and E-cadherin in tumors were significantly increased by antagomir-miR-181b tranfection and decreased by sh-p53 transfection; on the contrary, the Cyclin D1 protein level was reduced by antagomir miR-181b and increased by sh-p53 transfection (Fig. 6C).

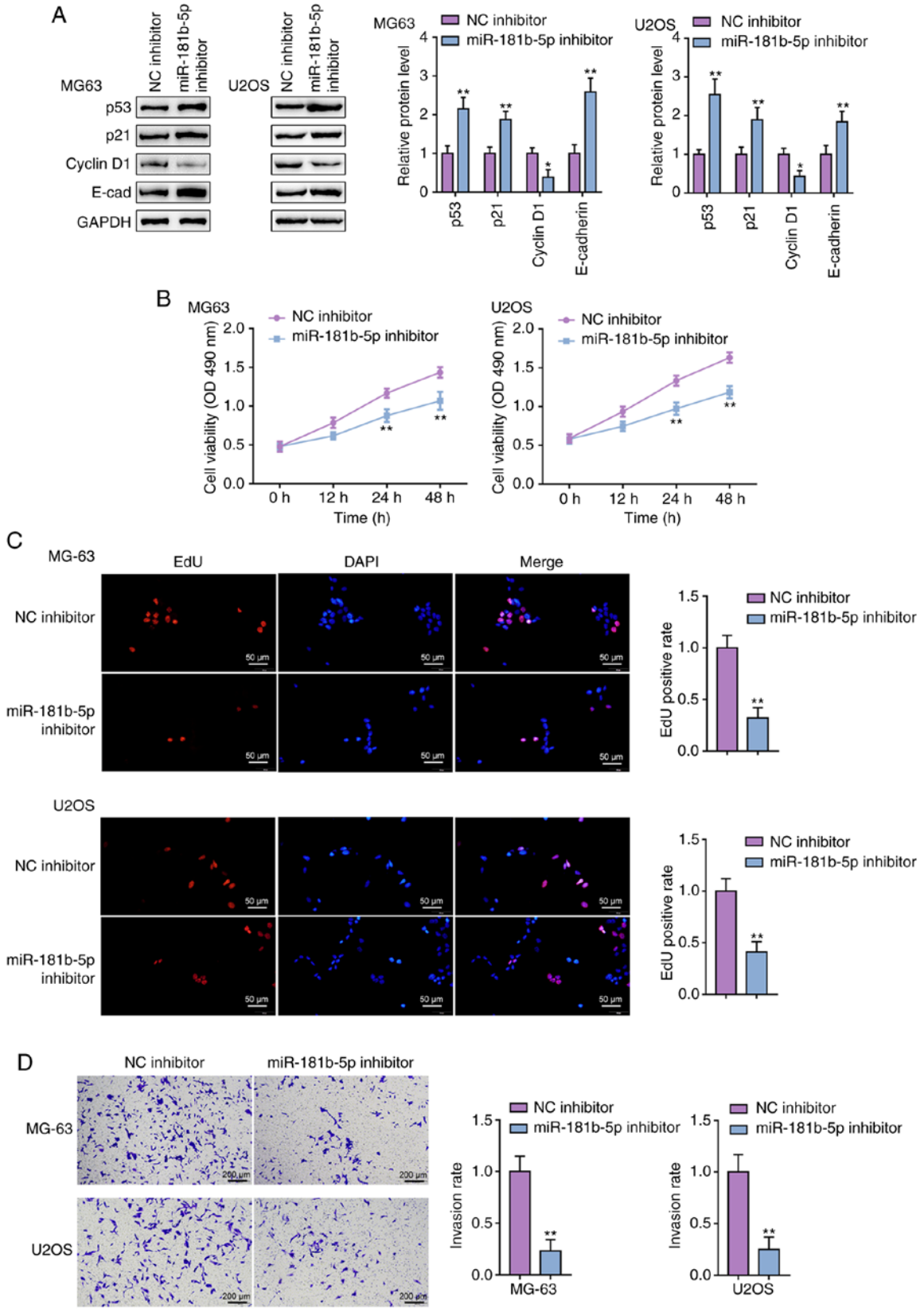

Figure 4. Detailed effects of miR-181b on p53 signaling and OS cell proliferation and invasion. MG63 and U2OS cells were transfected with miR-181b inhibitor and examined for (A) the protein levels of p53, p21, Cyclin D1 and E-cad by immunoblotting. (B) Cell viability by MTT assay. (C) The ability to synthesize DNA by EdU assay; and (D) invasive ability by Transwell assay. *P<0.05 and **P<0.01. E-cad, epithelial-cadherin; EdU, 5-ethynyl-2'-deoxyuridine; miR, microRNA; OS, osteosarcoma; NC, negative control; OD, optical density.

sh-p53 transfection significantly attenuated the effects of antagomir-miR-181b transfection (Fig. 6C). These results suggested that the miR-181b/p53 axis was involved in OS tumor growth in nude mouse model.

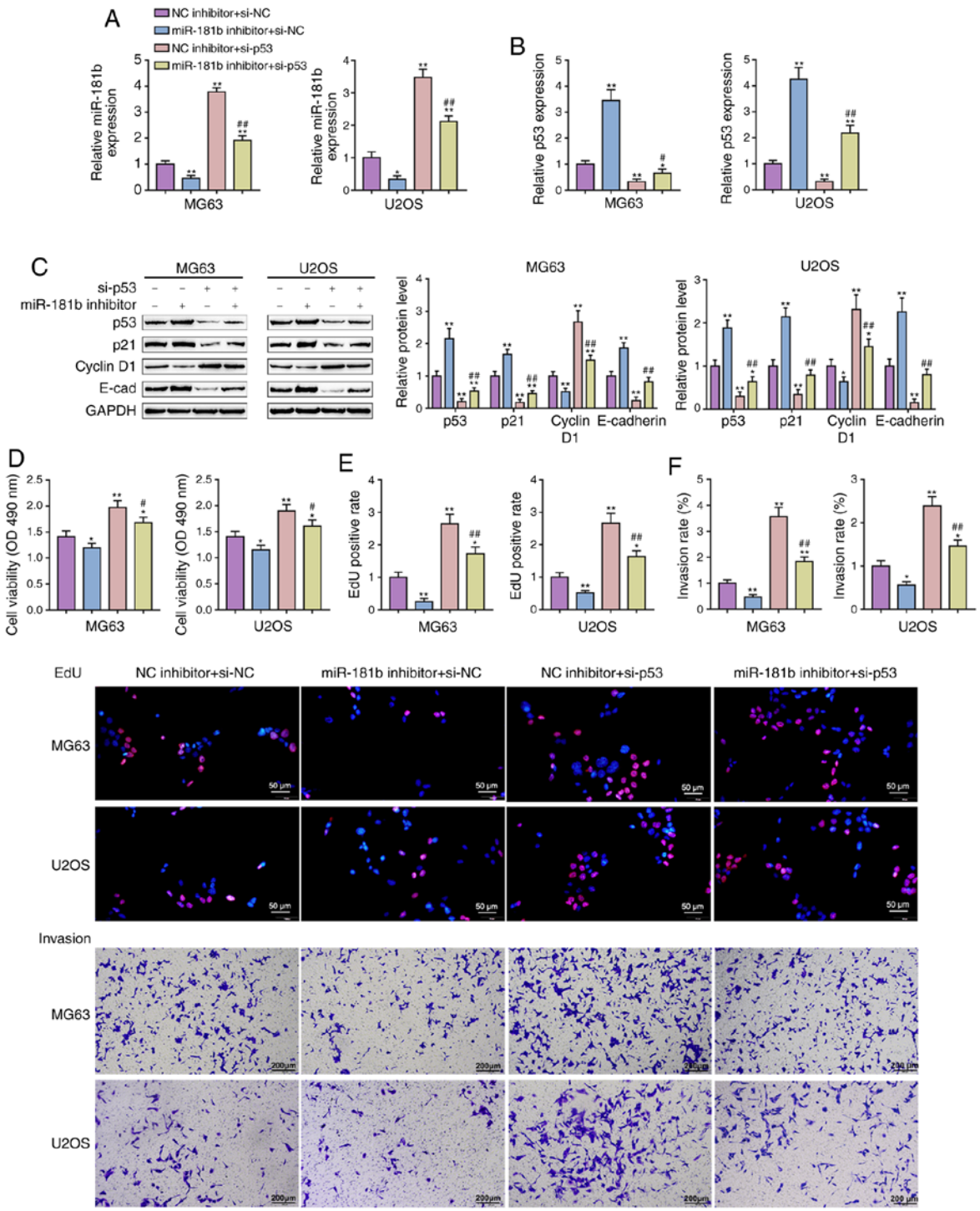

Figure 5. Dynamic effects of miR-181b and p53 on OS cell proliferation and invasion. MG63 and U2OS cells were co transfected with miR-181b inhibitor and si-p53 and examined for (A) the expression of miR-181b and (B) p53 by quantitative PCR. (C) the protein levels of p53, p21, Cyclin D1 and E-cad by immunoblotting. (D) Cell viability by MTT assay; (E) the ability to synthesize DNA by EdU assay and (F) invasive ability by Transwell assay. *P<0.05 and **P<0.01 vs. the NC inhibitor + si-NC group; $^{\#}$P<0.05 and $^{\#\#}$P<0.01 vs. the NC inhibitor + si-p53 group. EdU, 5-ethynyl-2'-deoxyuridine; miR, microRNA; OS, osteosarcoma; E-cad, epithelial-cadherin; si, small interfering; NC, negative control.

Discussion

In the present study, miR-181b expression was demonstrated to be upregulated whereas p53 expression was downregulated, within OS tissues and cells; in tissue samples, miR-181b and p53 were negatively correlated. p53 might inhibit the transcription of miR-181b via targeting its promoter region, whereas miR-181b bound the *TP53* 3'-UTR to inhibit p53 expression. The inhibition of miR-181b increased p53, p21 and E-cadherin protein levels but decreased Cyclin D1 protein levels in OS cells and OS cell xenografts; in addition, miR-181b inhibition reduced the capacity for OS cell proliferation and invasion both *in vitro* and *in vivo*. In contrast, p53 knockdown had opposite effects on these proteins and OS cell proliferation and invasion. Above all, p53 knockdown attenuated the effects of miR-181b inhibition.

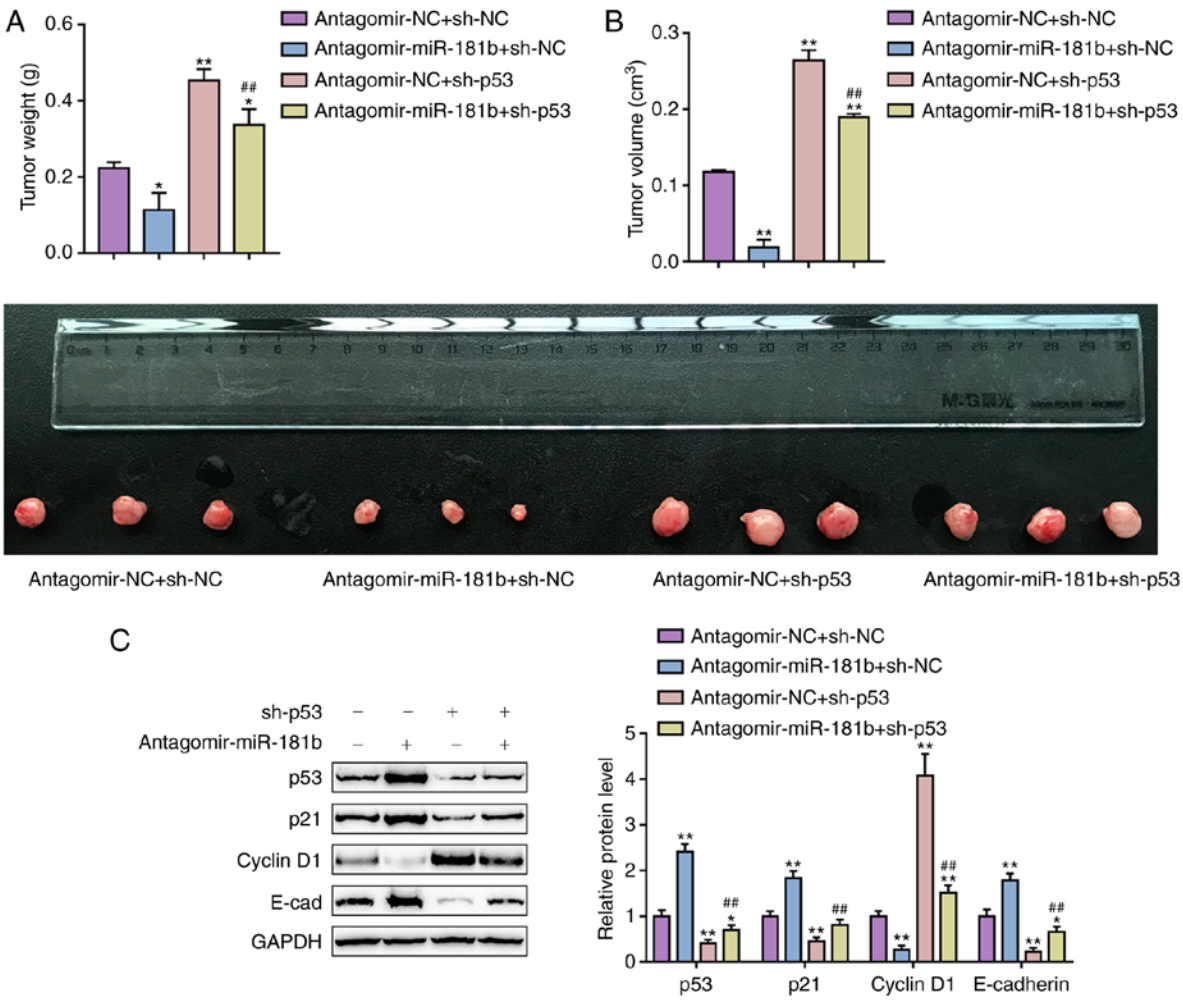

Figure 6. Dynamic effects of miR-181b and p53 on OS cell xenograft nude mice. OS cell xenograft (A) tumor weight and (B) tumor volume, and (C) the protein levels of p53, p21, cyclin D1, and E-cad in tumors from the antagomir-NC + sh-NC group, antagomir-miR-181b + sh-NC group, antagomir-NC + sh-p53 group and antagomir-miR-181b + sh-p53 group. The data are presented as the mean ± standard deviation of three independent experiments. *P<0.05 and **P<0.01 vs. the antagomir-NC + sh-NC group; $^{\#\#}$P<0.01 vs. the antagomir-NC + sh-p53 group. miR, microRNA; OS, osteosarcoma; E-cad, epithelial-cadherin; si, small interfering; NC, negative control; sh, short hairpin.

miR-181b was reported to be abnormally upregulated within various cancer types. The expression of miR-181b was increased within patient serum and breast cancer cells compared with those of healthy controls (30). Within OS cells, miR-181b OE induced, while miR-181b inhibition decreased the ability of OS cells to migrate and invade via directly binding NDRG2 (24). In the present study, consistent with previous studies, miR-181b expression was shown to be significantly enhanced, while the expression of p53, a well-established tumor suppressor (31,32), was decreased within OS tissue samples and cell lines.

TP53 can induce cell cycle arrest and apoptosis by regulating the transcription of miRNAs and other genes. p53 is regarded as mostly a transcriptional activator, but p53 has been revealed to inhibit specific gene expression in some reports (33,34). As demonstrated by studies on p53-mediated suppression, both genes that regulate apoptotic responses and genes that promote cell cycle progression can be inhibited via p53 (35,36). In the present study, both an online tool and experimental analysis indicated that p53 could directly bind miR-181b. p53 inhibited the transcription of miR-181b via targeting its promoter region. Interestingly, miR-181b also targeted TP53 at its 3'-UTR to inhibit p53 expression, thereby forming a negative feedback regulatory axis with p53. In OS cell lines, p53 and miR-181b were negatively regulated by one another. miR-181b was abnormally upregulated within OS cells, indicating that the overexpression of miR-181b might disturb the balance of the regulatory feedback axis to promote OS development.

To verify this speculation, the cellular effects of miR-181b and dynamic effects of miR-181b and p53 were further evaluated on OS cells. The oncogenic role of miR-181b has been widely reported. miR-181b downregulation within prostate cancer PC-3 cells induced apoptosis and suppressed PC-3 cell growth and invasion *in vitro* (37). miR-181b suppressed adenylyl cyclase 9 expression within cervical cancer cell lines to enhance cell proliferation and to inhibit apoptosis (38). Within colorectal cancer, miR-181b also bound PDCD4 to act as an oncomiR, promoting cancer cell proliferation and migratory capacity, suppressing apoptosis within CRC cells, and accelerating tumor growth within xenograft mice (39). In the present study, miR-181b inhibition enhanced p53, p21 and E-cadherin protein levels while decreasing Cyclin D1 protein levels. Apoptosis and growth arrest are the as two main endpoints

of p53 activation. Induction of the cyclin dependent kinase suppressor p21 may be essential for p53-mediated growth arrest. Consistently, miR-181b inhibition leads to a significant suppression upon the proliferation and invasion of OS cells, suggesting that the inhibition of miR-181b carries out its effects on OS cells via targeting p53 to modulate p53-mediated cancer cell growth arrest. As further confirmation, p53 knockdown had effects opposite to those of miR-181b inhibition on p53 signaling and OS cells. Moreover, the effects of miR-181b inhibition were reversed by p53 knockdown, indicating that abnormal miR-181b upregulation inhibited p53 and promoted OS cells proliferation and invasion. OS cell xenograft assays further confirmed the roles of miR-181b/p53 axis in OS growth.

In conclusion, miR-181b and p53 are negatively regulated by one another and therefore form a negative feedback axis that regulates OS cells proliferation and invasion abilites. Targeting miR-181b to inhibit its abnormal upregulation might be a potent strategy for OS treatment.

Acknowledgements

The authors would like to thank Mr Xin Liu from Central South University (Changsha, China) for his help with the xenograft nude mice experiments.

Funding

The present study was supported by the National Natural Science Foundation of China (grant no. 81301671).

Availability of data and materials

The analyzed datasets generated during the study are available from the corresponding author upon reasonable request.

Authors' contributions

JW, YL made substantial contribution to the conception and design of the study. FL, CZ analyzed and interpreted the data. JW, CZ drafted the manuscript; CZ, YL revised the work critically for important intellectual content. YL collected grants. All authors approved the final published version of this manuscript.

Ethics approval and consent to participate

All procedures performed in studies involving human participants were in accordance with the Ethics Committee of the Xiangya Hospital and with the 1964 Helsinki declaration. Informed consent to participate in the study was obtained from participants. The animal epxeriments were approved by the Ethic Committee of Xiangya Hospital of Central South University.

Patient consent for publication

Not applicable.

Competing interests

The authors declare that they have no competing interests.

References

1. Ma O, Cai WW, Zender L, Dayaram T, Shen J, Herron AJ, Lowe SW, Man TK, Lau CC and Donehower LA: MMP13, Birc2 (cIAP1), and Birc3 (cIAP2), amplified on chromosome 9, collaborate with p53 deficiency in mouse osteosarcoma progression. Cancer Res 69: 2559-2567, 2009.
2. Anderson ME: Update on survival in osteosarcoma. Orthop Clin North Am 47: 283-292, 2016.
3. Duchman KR, Gao Y and Miller BJ: Prognostic factors for survival in patients with high-grade osteosarcoma using the surveillance, epidemiology, and end results (SEER) program database. Cancer Epidemiol 39: 593-599, 2015.
4. Kedmi R, Veiga N, Ramishetti S, Goldsmith M, Rosenblum D, Dammes N, Hazan-Halevy I, Nahary L, Leviatan-Ben-Arye S, Harlev M, *et al*: A modular platform for targeted RNAi therapeutics. Nat Nanotechnol 13: 214-219, 2018.
5. Shaikh AB, Li F, Li M, He B, He X, Chen G, Guo B, Li D, Jiang F, Dang L, *et al*: Present advances and future perspectives of molecular targeted therapy for osteosarcoma. Int J Mol Sci 17: 506, 2016.
6. Papiol S, Arias B, Barrantes-Vidal N, Guitart M, Salgado P, Catalán R and Fañanás L: Analysis of polymorphisms at the tumor suppressor gene p53 (TP53) in contributing to the risk for schizophrenia and its associated neurocognitive deficits. Neurosci Lett 363: 78-80, 2004.
7. Li J, Yang L, Gaur S, Zhang K, Wu X, Yuan YC, Li H, Hu S, Weng Y and Yen Y: Mutants TP53 p.R273H and p.R273C but not p.R273G enhance cancer cell malignancy. Hum Mutat 35: 575-584, 2014.
8. Xie Y, Zhu S, Song X, Sun X, Fan Y, Liu J, Zhong M, Yuan H, Zhang L, Billiar TR, *et al*: The tumor suppressor p53 limits ferroptosis by blocking DPP4 activity. Cell Rep 20: 1692-1704, 2017.
9. Bedi A and Mookerjee B: Biological significance and molecular mechanisms of p53-induced apoptosis. Apoptosis 3: 237-244, 1998.
10. Xie C, Wu B, Chen B, Shi Q, Guo J, Fan Z and Huang Y: Histone deacetylase inhibitor sodium butyrate suppresses proliferation and promotes apoptosis in osteosarcoma cells by regulation of the MDM2-p53 signaling. Onco Targets Ther 9: 4005-4013, 2016.
11. Zhou Y, Niu W, Luo Y, Li H, Xie Y, Wang H, Liu Y, Fan S, Li Z, Xiong W, *et al*: p53/Lactate dehydrogenase A axis negatively regulates aerobic glycolysis and tumor progression in breast cancer expressing wild-type p53. Cancer Sci 110: 939-949, 2019.
12. Chen Z, Guo J, Zhang K and Guo Y: TP53 mutations and survival in osteosarcoma patients: A meta-analysis of published data. Dis Markers 2016: 4639575, 2016.
13. Luo Y, Deng Z and Chen J: Pivotal regulatory network and genes in osteosarcoma. Arch Med Sci 9: 569-575, 2013.
14. Zhao YX, Wang YS, Cai QQ, Wang JQ and Yao WT: Up-regulation of HDAC9 promotes cell proliferation through suppressing p53 transcription in osteosarcoma. Int J Clin Exp Med 8: 11818-11823, 2015.
15. Wu J, Guo A, Li Q and Wang D: Meta-analysis of clinical significance of p53 protein expression in patients with osteosarcoma. Future Oncol 13: 1883-1891, 2017.
16. Shukla GC, Singh J and Barik S: MicroRNAs: Processing, maturation, target recognition and regulatory functions. Mol Cell Pharmacol 3: 83-92, 2011.
17. Farh KK, Grimson A, Jan C, Lewis BP, Johnston WK, Lim LP, Burge CB and Bartel DP: The widespread impact of mammalian MicroRNAs on mRNA repression and evolution. Science 310: 1817-1821, 2005.
18. Pasquinelli AE, Hunter S and Bracht J: MicroRNAs: A developing story. Curr Opin Genet Dev 15: 200-205, 2005.
19. Jones KB, Salah Z, Del Mare S, Galasso M, Gaudio E, Nuovo GJ, Lovat F, LeBlanc K, Palatini J, Randall RL, *et al*: miRNA signatures associate with pathogenesis and progression of osteosarcoma. Cancer Res 72: 1865-1877, 2012.
20. Qin L, Chen Y, Niu Y, Chen W, Wang Q, Xiao S, Li A, Xie Y, Li J, Zhao X, *et al*: A deep investigation into the adipogenesis mechanism: Profile of microRNAs regulating adipogenesis by modulating the canonical Wnt/beta-catenin signaling pathway. BMC Genomics 11: 320, 2010.
21. Guo Y, Zi X, Koontz Z, Kim A, Xie J, Gorlick R, Holcombe RF and Hoang BH: Blocking Wnt/LRP5 signaling by a soluble receptor modulates the epithelial to mesenchymal transition and suppresses met and metalloproteinases in osteosarcoma Saos-2 cells. J Orthop Res 25: 964-971, 2007.

22. Zang X, Li Q, Wang W, Zhou Y, Chen S and Xiao T: miR-181a promotes the proliferation and metastasis of osteosarcoma cells by targeting RASSF1A. Zhong Nan Da Xue Xue Bao Yi Xue Ban 41: 789-795, 2016 (in Chinese; Abstract available in Chinese from the publisher).
23. Zhu ZJ, Huang P, Chong YX, Kang LX, Huang X, Zhu ZX and Nie L: MicroRNA-181a promotes proliferation and inhibits apoptosis by suppressing CFIm25 in osteosarcoma. Mol Med Rep 14: 4271-4278, 2016.
24. Shao JL, Li ZZ, Wang L, Jiao GL, Zhou ZG and Sun GD: microRNA-181b promotes migration and invasion of osteosarcoma cells by targeting N-myc downstream regulated gene 2. Nan Fang Yi Ke Da Xue Xue Bao 36: 321-326, 2016 (In Chinese).
25. Wang W, Wang Z, Chen S, Zang X and Miao J: Interleukin-1β/nuclear factor-κB signaling promotes osteosarcoma cell growth through the microRNA-181b/phosphatase and tensin homolog axis. J Cell Biochem 120: 1763-1772, 2019.
26. Kaste SC, Pratt CB, Cain AM, Jones-Wallace DJ and Rao BN: Metastases detected at the time of diagnosis of primary pediatric extremity osteosarcoma at diagnosis: Imaging features. Cancer 86: 1602-1608, 1999.
27. McCarville MB, Kaste SC, Cain AM, Goloubeva O, Rao BN and Pratt CB: Prognostic factors and imaging patterns of recurrent pulmonary nodules after thoracotomy in children with osteosarcoma. Cancer 91: 1170-1176, 2001.
28. Nolan T, Hands RE and Bustin SA: Quantification of mRNA using real-time RT-PCR. Nat Protoc 1: 1559-1582, 2006.
29. Liu ZB, Wang JA and Lv RQ: Downregulation of long non-coding RNA DBH-AS1 inhibits osteosarcoma progression by PI3K-AKT signaling pathways and indicates good prognosis. Eur Rev Med Pharmacol Sci 23: 1418-1427, 2019.
30. Zheng Y, Lv X, Wang X, Wang B, Shao X, Huang Y, Shi L, Chen Z, Huang J and Huang P: MiR-181b promotes chemoresistance in breast cancer by regulating Bim expression. Oncol Rep 35: 683-690, 2016.
31. Hong B, van den Heuvel AP, Prabhu VV, Zhang S and El-Deiry WS: Targeting tumor suppressor p53 for cancer therapy: Strategies, challenges and opportunities. Curr Drug Targets 15: 80-89, 2014.
32. Zhou J, Wu S, Chen Y, Zhao J, Zhang K, Wang J and Chen S: microRNA-143 is associated with the survival of $ALDH1^+CD133^+$ osteosarcoma cells and the chemoresistance of osteosarcoma. Exp Biol Med (Maywood) 240: 867-875, 2015.
33. Mack DH, Vartikar J, Pipas JM and Laimins LA: Specific repression of TATA-mediated but not initiator-mediated transcription by wild-type p53. Nature 363: 281-283, 1993.
34. Dickins RA, Hemann MT, Zilfou JT, Simpson DR, Ibarra I, Hannon GJ and Lowe SW: Probing tumor phenotypes using stable and regulated synthetic microRNA precursors. Nat Genet 37: 1289-1295, 2005.
35. Mirza A, Wu Q, Wang L, McClanahan T, Bishop WR, Gheyas F, Ding W, Hutchins B, Hockenberry T, Kirschmeier P, *et al*: Global transcriptional program of p53 target genes during the process of apoptosis and cell cycle progression. Oncogene 22: 3645-3654, 2003.
36. Spurgers KB, Gold DL, Coombes KR, Bohnenstiehl NL, Mullins B, Meyn RE, Logothetis CJ and McDonnell TJ: Identification of cell cycle regulatory genes as principal targets of p53-mediated transcriptional repression. J Biol Chem 281: 25134-25142, 2006.
37. He L, Yao H, Fan LH, Liu L, Qiu S, Li X, Gao JP and Hao CQ: MicroRNA-181b expression in prostate cancer tissues and its influence on the biological behavior of the prostate cancer cell line PC-3. Genet Mol Res 12: 1012-1021, 2013.
38. Yang L, Wang YL, Liu S, Zhang PP, Chen Z, Liu M and Tang H: miR-181b promotes cell proliferation and reduces apoptosis by repressing the expression of adenylyl cyclase 9 (AC9) in cervical cancer cells. FEBS Lett 588: 124-130, 2014.
39. Liu Y, Uzair-Ur-Rehman, Guo Y, Liang H, Cheng R, Yang F, Hong Y, Zhao C, Liu M, Yu M, *et al*: miR-181b functions as an oncomiR in colorectal cancer by targeting PDCD4. Protein Cell 7: 722-734, 2016.

This work is licensed under a Creative Commons Attribution-NonCommercial-NoDerivatives 4.0 International (CC BY-NC-ND 4.0) License.